AD-A258 708

‖‖‖‖‖‖‖‖‖‖‖‖‖‖

IMPROVED MODELS OF THE INNER AND OUTER RADIATION BELTS

K. A. Pfitzer

DTIC
ELECTE
NOV 12 1992
S A D

McDonnell Douglas Space Systems Co
Advanced Product Development & Technology
5301 Bolsa Avenue
Huntington Beach, CA 92647

August 1992

Scientific Report No. 2

92-29305

‖‖‖‖‖‖‖‖‖‖‖‖‖‖

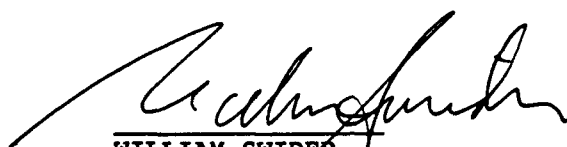"This technical report has been reviewed and is approved for publication"

KEVIN J. KERNS, Capt, USAF
Contract Manager

E. G. MULLEN
Branch Chief

WILLIAM SWIDER
Deputy Director

This document has been reviewed by the ESD Public Affairs Office (PA) and is releasable to the National Technical Information Service (NTIS).

Qualified requestors may obtain additional copies from the Defense Technical Information Center. All others should apply to the National Technical Information Service.

If your address has changed, or if you wish to be removed from the mailing list, or if the addressee is no longer employed by your organization, please notify PL/TSI, Hanscom AFB, MA 01731. This will assist us in maintaining a current mailing list.

Do not return copies of this report unless contractual obligations or notices on a specific document requires that it be returned.

REPORT DOCUMENTATION PAGE

Public reporting burden for this collection of information is estimated to average 1 hour per response, including the time for reviewing instructions, searching existing data sources, gathering and maintaining the data needed, and completing and reviewing the collection of information. Send comments regarding this burden estimate or any other aspect of this collection of information, including suggestions for reducing this burden, to Washington Headquarters Services, Directorate for Information Operations and Reports, 1215 Jefferson Davis Highway, Suite 1204, Arlington, VA 22202-4302, and to the Office of Management and Budget, Paperwork Reduction Project (0704-0188), Washington, DC 20503

1. AGENCY USE ONLY (Leave blank)	2. REPORT DATE August 1992	3. REPORT TYPE AND DATES COVERED Scientific Report No. 2

4. TITLE AND SUBTITLE

Improved Models of the Inner and Outer Radiation Belts

6. AUTHOR(S)

K. A. Pfitzer

5. FUNDING NUMBERS

PE 62101F
PR 7601 TA 22 WU MD

Contract:
F19628-90-C-0099

7. PERFORMING ORGANIZATION NAME(S) AND ADDRESS(ES)

McDonnell Douglas Space Systems Co.
Advanced Product Development & Technology
5301 Bolsa Avenue
Huntington Beach, CA 92647

8. PERFORMING ORGANIZATION REPORT NUMBER

9. SPONSORING/MONITORING AGENCY NAME(S) AND ADDRESS(ES)

Phillips Laboratory
Hanscom AFB, MA 01731-5000

Contract Manager: Lt. Kevin Kerns/GPSP

10. SPONSORING/MONITORING AGENCY REPORT NUMBER

PL-TR-92-2193

11. SUPPLEMENTARY NOTES

12a. DISTRIBUTION/AVAILABILITY STATEMENT

Approved for public release; distribution unlimited.

12b. DISTRIBUTION CODE

13. ABSTRACT (Maximum 200 words) In March 1991, after a very large sudden commencement, the CRRES satellite observed the creation of a large flux of high energy protons and electrons in the inner magnetosphere. A vector potential model of the time dependent Chapman-Ferraro currents is developed for this sudden commencement. This time dependent vector potential is then used to determine the magnetic field and the induction electric field during the sudden commencement. The model magnetic signature agrees well with the CRRES observations. The induction electric field calculated by the model ranges from 10s of milliVolts per meter at 3 Re on midnight side of the earth to as large as 400 milliVolts per meter on the noon meridian. The electric field is non-conservative and is capable of accelerating protons and electrons to many 10s of MeV. Sample proton trajectories are used to determine the acceleration of particles in the storm-time magnetic and electric fields. The appendix lists the complete FORTRAN code of the time dependent magnetic and electric field models.

14. SUBJECT TERMS

Induction electric field, Particle acceleration, magnetosphere, sudden commencement, magnetic storm, inner zone, magnetic field, models.

15. NUMBER OF PAGES
56

16. PRICE CODE

17. SECURITY CLASSIFICATION OF REPORT	18. SECURITY CLASSIFICATION OF THIS PAGE	19. SECURITY CLASSIFICATION OF ABSTRACT	20. LIMITATION OF ABSTRACT
Unclassified	Unclassified	Unclassified	SAR

Table of Contents

-iii-

y Codes

and / or
Special

A-1

1.0 Introduction

Considerable progress has been made in the understanding of magnetospheric processes in the last 25 years. During this time much of the effort has been focused on understanding processes operating in the tail of the magnetosphere and near the magnetospheric boundaries. The inner magnetosphere has not been extensively investigated in the last 10 to 20 years. The Combined Release and Radiation Effects Satellite (CRRES) Program is designed to make a substantial contribution to understanding this region of space.

In this effort McDonnell Douglas Space Systems Company (MDSSC) will introduce novel new modeling approaches and will satisfy one of main goals of the CRRES mission, the development of new static and dynamic radiation belt models. Such models are an important tool for engineers for the design of systems that can survive in the space environment. The present radiation belt models that are now used by both the scientific and engineering communities are the Vette radiation models developed by the National Space Sciences Data Center (NSSDC) in the late 1960's and early 70's. The data sets which were used to develop the Vette models were acquired by instruments that are quite primitive compared to today's state-of-the-art instruments. Nevertheless these older models have served the community well.

The present NSSDC developed models are organized in B, L space, a coordinate system developed by C. E. McIlwain in 1961 (McIlwain, 1961). This coordinate system has been virtually unchanged since that time. Improvements have come only in the form of improved computational techniques. Although the B, L system has proven useful in the inner zone, its use in the outer zone has not been as successful.

This CRRES analysis effort will include the development of new tools for the organization of the data. This effort will develop novel new techniques for organizing charged particle data in the inner and outer zone. In the inner zone we will develop a model that not only takes into account the effect of the magnetic field in organizing the charged particles but also the effect of the solar cycle dependent atmosphere in shaping the low altitude region of the inner radiation belt. In the outer zone we will provide a coordinate system that can correctly represent adiabatic changes in the radiation belt and fully take into account drift shell splitting and yet represent the entire outer zone in terms of only two parameters, an equivalent L and an effective equatorial pitch angle. Once the new tools developed under this effort are implemented and a best fit is made to the CRRES data, a high quality radiation belt model will be created that will be valid for all epoch within a solar cycle and for all magnetic conditions of the magnetosphere. In the inner zone, the new model will permit calculation of the fluxes during any part of the solar cycle. In the inner and outer zone the model will help separate adiabatic changes from non adiabatic variations, allow the calculation of particle fluxes for all states of magnetospheric compression, and will help theorists explain many of the observed changes within the magnetosphere.

One of the most important contributions of the CRRES satellite is its demonstration that the inner magnetosphere is considerably more dynamic than previously suspected. Many satellites have investigated the region in the tail and the region near synchronous orbit. The large variations in this region are much appreciated and have been the focus of numerous investigations. On the other hand the inner magnetosphere (below L = 3 or 4) has been ignored because of its apparent stability and lack of interesting 'events'. The March 1991 event, in which CRRES showed a very large permanent change to the inner radiation belt

came as a complete surprise to many. It should not have, except for the lack of a detailed study in this region of space.

The newly discovered dynamics of the inner radiation belt place an additional burden on the modeling techniques. In order to develop realistic models of the radiation environment, it is imperative that the processes that create the enhancements are understood. Since events such as the March 1991 event are very rare and isolated, a single event can be studied in considerable detail without contamination by other events. Furthermore, the size, of the particle energization, the size of the magnetic and electric fields make the identification of the various signatures more precise. This event is the first well-documented event in this class. It is now apparent that it is not the first and most certainly not the last event of its class.

Magnetic and electric field models as well as particle motion models are important tools in studying the dynamics of the inner magnetosphere. Some of the tools necessary to study this event were developed many years ago but were never needed or used. In particular, a vector potential model of the magnetospheric magnetic field developed almost 15 years ago was more of a curiosity since the magnetic field derived from it was not as accurate as a more direct model of the magnetic field. This vector potential model, does however, become an important tool in understanding the electric field during the March 1991 event.

The probability of understanding this event is much greater than understanding the sub-storm problem. Although, magnetic field variations are very large, several hundred nanotesla, and the electric field exceeds several hundred milliVolts/meter, the total magnetic field is over a thousand nanotesla in this region of space and thus the coordinate system as defined by the magnetic field

is relatively stable. This is very important simplification in our task of understanding the magnetosphere.

2.0 An Electromagnetic Model of the Magnetosphere During the March Event

The next sections describe the beginnings of a modeling effort that we believe has a very good probability of understanding a very important magnetospheric process using basic principles of physics.

2.1 A Vector Potential Model of the Magnetopause Current System

The first step in the development of the 1977 quiet-time Olson Pfitzer magnetic model was the definition of the current systems (Olson and Pfitzer, 1977). The magnetopause current system was represented by a set of triangular current sheets. The ring and tail currents were represented by a set of wire loops. An integration was then performed over the current systems to calculate both the magnetic field and the magnetic vector potential from the three current systems at a large number of points within the magnetosphere. The integration effort produced a set of files containing the magnetic field and the vector potential at a large number of locations for various dipole tilt values. Orthonormal function fitting techniques were then used to derive functional forms for both the vector potential and the magnetic field. The curl of the vector potential model was then compared to calculated magnetic field values. The curl of the vector potential gave a magnetic field that was a reasonable representation of the calculated magnetic field values. However, the functions determined directly from the magnetic field values produced a magnetic field model that was considerably superior to the magnetic field model using the curl of the vector potential model. We thus decided to set aside the vector potential model and published the functional form of the direct fit magnetic field model. This became the much used 1977 tilt dependent model for quiet time. This model is valid to 13 Re and

has been used extensively by many researchers. It has been extensively validated and found to have considerable precision during quiet times.

A somewhat later effort used the above described vector potential model to study the magnetic and electric field variations from the wobbling dipole. The induction electric field calculated from the tilt dependent vector potential was used to study possible particle accelerations due to the wobbling dipole. This effect proved to be quite small, although non-trivial. The vector potential model was thus relegated to dark deep desk drawer.

It is this vector model, developed almost 15 years ago, that was the starting point for the present analysis. One should remember that the current systems that are used for its definition are the same current systems that are used for the highly successful 1977 magnetic field model. The original vector potential model developed in 1977 contained the effects of all of the current systems and thus the functions used in the fit are unnecessarily complicated for this work. For the study of the acceleration due to the changing magnetopause currents, one should use only the magnetopause currents. It was possible to easily separate the coefficients for the magnetopause currents. Redefining the functional form to remove terms that help fit the ring current would have been very labor intensive. Although simpler functions would increase computational efficiency and accuracy, the precision required for this initial study did not justify this additional work. Thus the vector potential model used for this study consist of a set of polynomials and polynomials times an exponential that has virtually the same form as the 1977 magnetic field model. The coefficients for the model are the coefficients derived from the magnetopause currents. As discussed above, the accuracy of this vector potential model was validated in 1977 when the curl of the vector potential was compared point for point against the magnetic field

values calculated from the current systems and the total calculated magnetic field was compared to the delta B contours of Sugiura (Sugiura, et. al., 1971). The vector potential model listed in Appendix A is thus a high fidelity model of the vector potential developed from the 1977 tilt dependent model and specifically modified for this effort to include only the magnetopause currents.

2.2   Extending the Vector Potential Model to Disturbed Times

The vector potential model developed from the 1977 tilt dependent current system is only valid during quiet time. This model was extended for use during disturbed times using techniques developed during the Consolidated Data Analysis Workshops (CDAW). Extensive work with the various (CDAW) data sets validated a method of extending a quiet time model to disturbed times. This method has been shown to work particularly well for scaling the magnetopause currents in response to changes in the stand-off distance. The justifications for the scaling techniques are discussed in Olson and Pfitzer 1982. This same scaling technique can be applied to the vector potential model.   Appendix A describes a FORTRAN code for a quiet time magnetopause vector potential model, a disturbed vector potential, a quiet time magnetic field as derived from the curl of the vector potential and a disturbed magnetic field model as calculated using the curl. Appendix A also describes the algorithms for extending the quiet time model to disturbed times.

2.3   The Induction Electric Field

the great advantage of a vector potential model is that one can calculate the Induction electric field directly. The induction electric field, E_I, is given by

$$E_I = -\frac{\partial A}{\partial t}$$ (1)

Note that all work in this analysis is performed in MKS units.

To calculate the time dependent electric field one must have a time dependent vector potential. The vector potential routines described in Appendix A give the vector potential as a function of the standoff distance. Thus a time dependent standoff distance will produce a time dependent vector potential. This vector potential can then be used to calculate a time dependent induction electric field.

2.4 Pressure Balance During the March 1991 Event

To develop a model for the magnetic field and for the induction electric field during the large sudden commencement of March 1991, we need a time history of the solar wind pressure during the event. Unfortunately very little solar wind information is available for this event. We thus assume that before the sudden commencement, the solar wind pressure was nominal and that the standoff distance was at 10.5 Re. We also assume that there was a discontinuous change in the solar wind pressure, a step function in the solar wind pressure. Travel times of the solar wind plasma from sun suggest that the velocity of the shock during the March 1991 event was on the order of 1450 km/sec. We further assumed that the magnetopause was compressed to a minimum distance of about 5 Re. The magnetopause cannot instantly respond to a pressure discontinuity and thus some time is required for the standoff distance to change from 10.5 to 5 Re. The time dependent standoff distance function was first developed such that the calculated magnetic signature matched the signature observed by the CRRES magnetometer. The CRRES magnetometer sees a positive dB/dt lasting for approximately 30 seconds (see figure 1). Thus, the initial work assumed that the standoff distance moved from 10.5 Re to 5 Re in 30 seconds. The time rate of change of the standoff distance change was

-8-

assumed to be nonlinear. Since the magnetic field becomes stronger as the field is compressed, the rate of change of distance should slow down as the boundary moves in. Several functional forms were constructed. The final function was selected on the basis of correctly modeling the dB/dt observed by the CRRES magnetometer. The function that was found to give an acceptable result has the form,

$$R_s = 10.5 \cdot \left[1 + 9 \cdot \left(\frac{t}{30} \right)^{1.3} \right]^{-1/3}$$

(2)

where R_s is the standoff distance and t is the time since the start of the event. Figure 2 gives the time dependent standoff distance predicted by the above equation. Using this standoff distance function for the vector potential model gives a dB/dt at the location of CRRES as shown in figure 3. This compares very favorably with the CRRES data shown in figure 1.

The above determined of rate-of-change of standoff distance has no theoretical foundation. George Siscoe of UCLA (private communication) noted that during a sudden change in solar wind pressure, the magnetosphere must remain in equilibrium at all times. That is, when the solar wind pressure changes, the magnetospheric boundary must move so as to maintain pressure balance during the motion. The velocity term in the pressure balance equation is not the velocity of the solar wind, but the difference in the velocity of the solar wind and the velocity of the moving boundary. Thus

$$R_s = 98 \cdot \left[\rho V^2 \right]^{-1/6}$$

(3)

where V is the velocity difference between the solar wind speed and the velocity of the boundary. The constant 98, is the constant that was developed for our dynamic magnetic field models. This can be rewritten to give

$$V = \frac{1}{\sqrt{\rho}} \left[\frac{98}{R_s} \right]^3 \tag{4}$$

Thus

$$v_s + \gamma \frac{\partial r}{\partial t} = \frac{1}{\sqrt{\rho}} \left[\frac{98}{r} \right]^3 \tag{5}$$

where v_s is the solar wind velocity, $\partial r / \partial t$ is the velocity of the boundary, γ is 6371 and changes the boundary velocity from units or R_e/sec to km/sec, r is the instantaneous position of the boundary. This gives rise to the following simple differential equation

$$dt = \frac{\gamma r^3 \, dr}{\frac{98^3}{\sqrt{\rho}} - v_s r^3} \tag{6}$$

This can be written as an easy to solve integral

$$t = \gamma \int_{10.5}^{R_s} \frac{r^3 dr}{a + br^3} \tag{7}$$

where $a = 98^3 / \sqrt{\rho}$ and $b = - v$

Evaluating the integral gives

$$t = \frac{r}{a}\bigg|_{r=10.5}^{r=R} - \frac{k}{3b} \left[\frac{1}{2} \ln \frac{(k+r)^2}{k^2 - kr + r^2} + \sqrt{3} \tan^{-1} \frac{2r-k}{\sqrt{3}k} \right]\bigg|_{r=10.5}^{r=R_s} \tag{8}$$

where $k^3 = a/b$

This gives the time, t, since the start of the arrival of the solar wind pressure change as a function of the instantaneous location of the standoff distance R_s. Since no value was available for ρ the solar wind number density, we used a value of 30 which is consistent with a minimum standoff distance of 5 at a solar

wind velocity of 1450 km/sec. Substituting values into the above equation gives the time dependent standoff distance as a function of time determined using dynamic pressure balance. The result of this dynamic pressure balance analysis is given in figure 4. We note with interest that this figure is very similar to figure 2. Figure 2 is determined by attempting to fit the CRRES magnetometer observations and figure 4 attempts to use a more theoretical approach. Both methods could be substantially improved if actual measurements become available of the real solar wind velocity and particle density during this event. This analysis is, however, consistent enough to allow us some confidence that either figure 2 or 4 can be used as the starting point for the development of a time dependent vector potential. For this report we have used the much simpler form (equation 2). The time dependent vector potential is driven by the time dependent standoff distance. This allows us to investigate the induction electric field created by the change in location and the change in strength of the Chapman Ferraro currents. During this compression, the Chapman Ferraro currents move inward from 10.5 to 5.5 R_e and increase in strength by an order of magnitude in a time period of approximately 30 seconds.

2.5   Magnetic signature During the March Event

Figure 3 gives the derivative of the magnetic signature determined by the time dependent magnetopause model. The integral of this magnetic field change, the amplitude of actual delta **B** spike predicted by the model at the location of CRRES, is 75 nanotesla. At 2.7 R_e on the noon meridian, the delta **B** spike is predicted to be 240 nanotesla. At the surface of the earth, the magnetic field spike should vary from 120 nanotesla at midnight to 170 nanotesla at local noon. Mid-latitude magnetometers may see a magnetic field spike that will exceed this magnitude due to currents induced in the earth. The induction currents due to

-11-

the conducting earth may increase the magnetic field signature as much as 60 percent. The exact enhancements have not yet been calculated. We understand the size of the increases to the S_q signatures that have a period of 24 hours. It is not prudent, however, to apply the same increase to a change with the period of 30 seconds. In order to determine the induction currents in the surface of the earth one must solve the problem of a magnetized conducting sphere with finite conductivity during a 30 second magnetic field pulse. This is a non-trivial problem that may require extensive analysis.

2.6   The Induction Electric Field During the March Event

The time dependent standoff distance given in figure 2 was used to calculate the induction electric field during this event at various locations within the magnetosphere. Figure 5 gives the induction electric field at CRRES during the 30 second compression period. One notes the rapid rise in the electric field to a level of approximately 50 mV/m. The present model only represents the period of active inward motion. At the end of the compression period the electric field will rapidly decay to zero and then actually reverse since the magnetosphere relaxed somewhat after the initial compression (see figure 1). Figure 6 gives the induction electric field on the local noon meridian at a distance of 2.7 Re from the center of the Earth. One notes that this field increases to almost 400 mV/m. The rate of change of the induction electric field in figure 6 differs from the rate of change seen in figure 5. This is due to the fact that figure 6 is on the noon meridian and much closer to the approaching currents. The electric field at this location is due not only to the increasing strength of the Chapman-Ferraro currents but also to the rapidly approaching currents. CRRES which is toward the dark side of the earth is farther from the currents and thus is most sensitive to changes in the strength of the Chapman-Ferraro currents. Figure 7 is a

snapshot of the electric field in the equatorial plane at time t = 20 seconds. At this time the magnetopause boundary is passing through 6.0 R_e. The induction electric field is given every 1.0 R_e on a rectangular grid. The length of the line is proportional to the strength of the field. A line .5 R_e long corresponds to a field value of 500 mV/m. The direction of the line gives the direction of the induction electric field vector. The dot at the end of the line points in the positive field direction. We note that the field is in most places tangent to the azimuthal direction and that the direction of the field on the sunlit side is such that both electrons and protons will experience a large gain in energy. There will be deceleration near local midnight, but this is small since the field is much smaller in this region. Once the compression of the magnetic field stops and the magnetosphere relaxes the electric field pattern will reverse its direction. From the magnetometer data in figure 1, one can see that only a partial relaxation occurs and thus the deceleration fields will be weaker. Furthermore any particle that was near noon during the start of the acceleration will most likely be near local midnight during the deceleration phase and will thus be shielded from the deceleration phase. The induction electric field is a non-conservative field. Even if the acceleration and deceleration fields were equal and opposite, some of the particles would experience substantial permanent acceleration. There would of course be a class of particles that would experience permanent deceleration.

2.7 The Parallel Electric Field

Because of symmetry, the induction electric field from the magnetopause currents is perpendicular to the magnetic lines of force in the magnetic equatorial plane. At all other locations there is a component of the induction electric field that is parallel to the field lines. Since the conductivity along field lines is very high, there will be a very rapid redistribution of charges along the line of force

such that the total electric field parallel to the lines of force is zero. The total electric field is given by

$$\mathbf{E}_T = -\frac{\partial \mathbf{A}}{\partial t} - \overline{\nabla}\Phi \qquad (9)$$

$-\overline{\nabla}\Phi$ is the scalar potential electric field is due to charge separation. Charges will realign themselves such that the parallel component of $\mathbf{E}_T$ is everywhere zero. This charge rearrangement which cancels the parallel portion of the total field can substantially modify the electric field perpendicular to the lines of force.

It is possible to calculate the charge separation electric field. During our work with the induction electric field due to wobbling dipole we developed a routine that performed a line integral along a line of force into the ionosphere. The total electric field along this line of force was required to remain zero everywhere along the line of force. This required introducing a potential variation along the line of force so that the gradient of the potential along the line of force would everywhere cancel the parallel component of the induction electric field. Adjacent line integrals can then give the gradients of the potential electric field perpendicular to the lines of force. Since potentials are arbitrary to within a constant, the analysis depends on the correct use of the boundary condition. Since the foot of the field line is anchored in the conducting ionosphere, the ionosphere becomes the physical boundary condition. During our wobbling dipole analysis we used either an equipotential ionosphere or an ionospheric boundary condition that assumed that the earth was a rotating conducting magnetized sphere.

A similar analysis will be instructive in this case. This part of the electric field analysis has not yet been completed. It is the intention to place a high priority on this analysis. During our wobbling dipole analysis, the induction electric field was

-14-

very small and the difference between the two boundary conditions was very large. Since the driver induction electric field for this event is two orders of magnitude greater than that of the wobbling dipole field, we expect less sensitivity to the form of the ionospheric boundary condition. We do, however, expect a substantial change in the overall electric field pattern. In many cases, canceling the parallel electric field may substantially increase the perpendicular electric field.

3.0 Particle Acceleration

Since the electric field is approximately azimuthal in the equatorial plane one can make a quick estimate of the amount of energy gain that one can expect for protons and electrons. The energy gain is simply the $E \cdot dl$. Estimating the path length from local dawn to dusk or dusk to dawn and multiplying by approximately 400 mV/m gives an approximate energy gain of 20 MeV at R =2.7 and 30 MeV at R = 4. These are very large numbers and suggest that the induction electric field due to the Chapman Ferraro currents is very important in understanding the particle energization that CRRES observed during the March 1991 event.

3.1 Lorentz Force

The force on a charged particle is given by

$$F = q (E + v \times B) \tag{10}$$

A modified cosmic ray trajectory code was used to integrate the trajectory of protons using equation 10. The initial cosmic ray code used by many investigators was modified to step in time instead of position. It was modified to include the effects of the electric field and energy conservation was removed from the code. The code can perform on the order of 50,000 integration steps before round off errors begin to affect the accuracy of the code. Thus proton motion during the event can easily be studied. However, the motion of electrons cannot easily be studied by a trajectory integration program. To study electron motion a guiding center code must be used. For this analysis only proton trajectories were studied.

3.2 Particle Motion During the March Event

A Lorentz force trajectory code is very attractive because of its simplicity. Cosmic ray codes have been extensively verified and shown to be accurate. The Lorentz force equation includes all effects. For our analysis we used the electric field as given by the induction electric field due to the changing Chapman-Ferraro currents. The electric field is calculated from the time dependent vector potential. Similarly the magnetic field consists of a dipole field plus the time dependent magnetic field calculated from the curl of the same time dependent vector potential. The magnetic and electric field codes are described in Appendix A. An overview of the Lorentz force integration code is given in Appendix B. The summary of the Lorentz force code is presented in Appendix B for reasons of completeness. The listing of the code will allow the user to easily verify the results of the analysis presented in this document.

To perform the actual analysis, the trajectory code was reversed and a negative proton was integrated backward in time. This allows us to begin the study at the point of observation and determine the initial starting point of the particle at time zero. One of the important milestones in the analysis of the March event will be the development a model of particle motion and acceleration that can show the origin of the particles seen by the CRRES spacecraft. Are the particles accelerated from the local population or are they accelerated inward from the cosmic ray flux in the outer zone?

Figure 8 shows a sample trajectory calculation. The particle was started at approximately 3 R_e and 3 hours local time with an energy of 50 MeV and a pitch angle of 90 degrees. The particle was started at time t = 30 seconds. At time t = 0 seconds the proton was at a local time of 21 hours and had an energy of 10

MeV and was at a radial distance of 4.5 R_e. Thus during the 30 seconds of positive dB/dt, this test particle drifted through 270 degrees. From Figure 7 one can see that almost the entire drift period was in a region where the electric field was in a direction necessary for acceleration. Many other trajectories were analyzed. The amount of energy gain is strongly associated with the drift velocity. The particle whose drift velocity is such that it drifts at least 180 degrees in 30 seconds shows the largest amount of energy gain. Very low energy particles have very low drift velocities and thus their $E \cdot dl$ is very small since the drift path length in 30 seconds is short. These particles will also be decelerated by the relaxation of the boundary after the initial increase. The particles with fast drift velocity will have drifted to the night side of the earth where the deceleration effect is small, but the slow particles will still be on the dayside and will experience the full deceleration.

Table 1 is a summary of results. The table lists starting and ending Ls as well as starting and ending energies. From this table one can see that energy gain is larger at higher energies and that the energy gain is larger at larger distances. Furthermore, the change in L is less for the smaller L shells. A quick investigation of this table shows that protons with a final L shell of 2.4 originated from Ls in the vicinity of 3.0 Re. These protons most likely originate from the existing trapped proton flux. Protons with a final L of 3.0 originate from Ls greater than 4.5 and could thus have their origin in the solar proton flux present in the outer zone at this time.

The results in Table 1 are all for particles with a pitch angle of 90 degrees. Several trajectories were run for non 90 degree particles. It is apparent from these runs that the energy gain is in the component of energy perpendicular to the magnetic field. Thus this acceleration mechanism will produce particles with

a pitch angle spectrum peaked near 90 degrees and thus the newly created belt will be must stronger near the equator.

4.0 Discussion and Summary

This report details the first steps in developing a storm time model of the magnetic and electric fields during a very large sudden compression of the magnetosphere. We believe that the model of the Chapman-Ferraro currents for this event is a good approximation for this event. Two separate techniques, one based on reproducing the CRRES magnetic signature, and one based on maintaining dynamic equilibrium during compression give approximately the same result. The biggest uncertainty is in the actual solar wind pressure parameters.

One fundamental simplification has been made in the analysis of the Chapman-Ferraro currents. In the analysis we assume that the entire magnetosphere responds as a unit. The entire magnetosphere contracts at the same time and at the same rate, and the entire current system increases its value uniformly over the entire magnetopause. In reality, the front of the magnetopause will change first with the more distant tail currents responding much later. However, the most important currents, the currents that dominate the magnetic signature in the region of interest (the inner magnetosphere), are within a few R_e of the sub solar point. Thus this approximation does not introduce a very large error. The biggest error in the analysis to date is that we have assumed a vacuum magnetosphere. We have not yet included the effect of the plasma within the magnetosphere. An additional complication of a non-vacuum magnetosphere is that the electromagnetic disturbance created by the changing Chapman-Ferraro currents will propagate with a finite speed, most likely the Alfven speed. This may introduce delays in the arrival of the disturbance vector proportional to the distance from the sub solar point. This propagation delay should be on the order of 10s of seconds and thus should be measurable by using timing marks at

-20-

various magnetometer locations on satellites and on the ground. The rise time of the event is very sharp and thus delay time measurements with an accuracy of seconds can reasonably be expected. Furthermore, since CRRES measures both the magnetic and electric field disturbances, it should be possible to easily calculate the direction of the propagation vector of the disturbance pulse.

This event offers a unique opportunity for investigating the injection of particles into the trapping region using only Maxwell's equations. The injection is in a region where the magnetic field is strong and the magnetic coordinate system not extensively distorted. CRRES is in the very center of the injection region. The magnetopause vector potential model provides an excellent first look insight into the energy that is available from the changing magnetopause current system. The first look energization shown in Table 1 show that more than enough energy is available and that the injection mechanism is the induction electric field. One must now solve the very complex details of the problem. Two of the most important details are the fact that the magnetosphere does contain a plasma and that the electromagnetic wave does have a finite propagation velocity. One of the first priorities during the next year of this effort will be the reevaluation of the electric field using the $\mathbf{E} \cdot \mathbf{B} = 0$ condition. We expect that including this effect in the electric field model will change the electric field pattern and that the electric field perpendicular to the magnetic lines of force will be increased.

The CRRES data set in conjunction with various other data sets are of sufficient quality to greatly assist in the development of a complete model of this unique event. The final model of the March 1991 event will be an important milestone in the understanding of magnetospheric dynamics.

5.0 Appendix A

This appendix describes and lists a series of subroutines that describe the magnetic and electric fields during the March 1991 event.

5.1 Subroutine AXYZ

This subroutine is the basic vector potential subroutine. The routine was developed in 1977 along with the 1977 Olson Pfitzer tilt dependent magnetic field model. The routine calculates the magnetic vector potential in units of nanotesla-Re everywhere inside the magnetosphere and inside of a sphere of radius 13 Re. The routine is tilt dependent. The routine is a series of polynomials plus polynomials times an exponential. The complexity of the function is such that if the coefficients of the ring and tail are added to coefficients describes in this listing, the functions have sufficient fidelity to describe the detailed structure due to the ring and tail current systems.

5.1.1 Calling sequence

XX(3)   a 3 dimension input array that specifies the position in Cartesian solar magnetic coordinates. XX(3) along the north dipole axis, XX(1) is perpendicular to XX(3) and in the plane containing XX(3) and the sun-earth line and pointing in the direction of the sun, XX(2) completes the right handed coordinate system. The distance are given in unit of Re.

AT(3)   a 3 dimensioned array that returns the vector components of the magnetic vector potential. The units are in nanotesla-Re.

COMMON/TILTIT/TILT   TILT is an input variable that specifies the tilt of the earth's dipole axis. Zero tilt indicates that the dipole is perpendicular to the sun-earth

line. Positive tilt is when the northern dipole is tipped toward the sun. This value must be set up before a call is made to routine AXYZ.

5.1.2 Program Listing - Subroutine AXYZ

```
      SUBROUTINE AXYZ(XX,AT)
C This routine caluclates the Vector potential of the magnetopause
c magnetospheric magnetic field during quiet conditions for any tilt.
C XX(3) is a real*8 position in earth radii in solar magnetic coords
C AT(3) is the real*8 vector potential in nanotesla-Re
      REAL*8 TILT
      REAL*8 D(44),E(64),F(44),DM(88),EM(128),FM(88),
     *AT(3),X(10),Y(10),Z(10),XX(3),TT(4),AA(3),
     *TILTL,XN,YN,ZN,R2,R
      INTEGER*2 ITD(44),ITE(64),ITF(44),
     *I,II,K
      COMMON/TILTIT/TILT
      DATA ITD /1,2,1,2,1,1,2,1,1,1,2,1,2,1,1,2,2,1,2,1,1,1,1,2,1,2,1,1,
     *2,1,1,1,2,1,2,1,1,2,2,1,2,1,1,1,1/
      DATA ITE /1,2,1,2,1,1,2,1,1,1,2,1,1,2,1,1,2,2,2,2,2,1,2,1,1,1,1,2,
     *1,1,1,2,1,2,1,2,1,1,2,1,1,1,2,1,1,2,1,1,2,2,2,2,2,1,2,1,1,1,1,2,1,
     *1,1,2/
      DATA ITF /2,1,2,1,2,2,1,2,2,2,1,2,1,2,2,1,1,2,1,2,2,2,2,1,2,1,2,2,
     *1,2,2,2,1,2,1,2,2,1,1,2,1,2,2,2/
      DATA (DM(I),I=1,88)/
     *-.729348268D+00,-.126711994D-03,-.250256245D-02,-.929734000D-06,
     *-.651629108D-01,-.166931408D-04,-.429000833D-03,-.274123969D-07,
     *-.313618130D-02,-.569972419D-05, .101581273D-02, .210875857D-05,
     * .100224170D-04, .447416904D-08, .157165005D-04, .371435608D-07,
     *-.302681932D-03, .526556403D-06, .139932388D-03, .163943276D-06,
     * .236910507D-05, .404562068D-09,-.174908288D-02, .111043613D-05,
     * .395551400D-05, .196463764D-07,-.172010105D-04, .104333857D-06,
     * .328361431D-05,-.381150320D-08, .188742505D-05, .796065264D-08,
     * .344430885D-06, .133982119D-08, .245745657D-03, .220385117D-06,
     * .245904885D-05, .986230049D-09, .183409240D-04, .265129601D-07,
     *-.212837026D-05,-.872199184D-08, .172169713D-04, .294076230D-08,
     *44*0./
      DATA (EM(I),I=1,128)/
     * .539534465D+01,-.917246729D-03,-.202212227D-02,-.129650634D-05,
     * .848876852D+00, .710329502D-04, .305008723D-02, .120551460D-05,
     *-.598376603D-01,-.165177282D-06,-.334958332D-02, .472213553D-05,
     * .422206531D-04, .173170587D-07, .160966776D-03, .208088996D-08,
     * .201674318D-02, .869926096D-05,-.170424338D-02,-.280163907D-05,
     *-.741748071D-05,-.919757909D-08,-.426006943D-05,-.533888339D-07,
     * .459399443D-01, .163072391D-04, .445957685D-03, .511926130D-08,
     * .562030059D-03,-.263083865D-06,-.400241568D-04,-.228038044D-06,
     *-.265641610D-05,-.173364107D-09,-.111586849D-03, .487350690D-07,
     * .558513796D-06,-.355505259D-09,-.173441325D-04,-.139197938D-08,
     * .149384635D-05,-.184142610D-08,-.565550702D-03,-.127131636D-05,
```

```
     *-.377826457D-05,-.241832155D-07, .395029200D-04,-.150796074D-06,
     * .141863427D-04, .157547770D-07,-.894741777D-05, .441400372D-07,
     * .869472657D-05,-.170170836D-07,-.123151650D-06,-.675272345D-10,
     *-.549566250D-04,-.134417266D-07, .538339684D-05, .119398067D-07,
     *-.105866429D-03,-.224420771D-06,-.298911521D-05,-.432303236D-09,
     *64*0./
      DATA (FM(I),I=1,88)/
     * .452063859D-02, .309321235D-06, .658118267D-01, .922543691D-05,
     * .221930272D-03,-.269376799D-06, .434366116D-02,-.169477296D-05,
     * .264268049D-03,-.496539062D-07,-.383052388D-04,-.818745994D-08,
     *-.139054930D-03,-.902753036D-07,-.122044254D-05, .305995114D-09,
     * .299405601D-05,-.823980252D-08,-.137081926D-06, .686745107D-09,
     *-.449407954D-05, .516272489D-08,-.108807156D-03,-.225109712D-07,
     *-.387313966D-03,-.181461377D-06,-.257814468D-05, .362172735D-09,
     * .107887529D-05,-.817801019D-10, .327270756D-04,-.213768490D-06,
     * .182395159D-04,-.467691071D-07,-.425729821D-05, .457564728D-08,
     *-.507417182D-04, .234472682D-07,-.828838728D-06,-.222432842D-09,
     * .118487595D-06, .259558968D-10, .445023379D-06, .345792292D-09,
     *44*0./
      DATA TILTL/99.D+0/
      IF(TILT.EQ.TILTL)GO TO 20
      TILTL=TILT
      TT(1)=1.
      TT(2)=TILT
      TT(3)=TILT*TILT
      TT(4)=TT(3)*TILT
      DO 10 I=1,64
      II=(I-1)*2+1
      K=ITD(I)
      if(i.le.44)D(I)=(10.*DM(II))*TT(K)+(10.*DM(II+1))*TT(K+2)
      K=ITE(I)
      E(I)=(10.*EM(II))*TT(K)+(10.*EM(II+1))*TT(K+2)
      K=ITF(I)
10    if(i.le.44)F(I)=(10.*FM(II))*TT(K)+(10.*FM(II+1))*TT(K+2)
20    CONTINUE
      XN=XX(1)
      YN=XX(2)
      ZN=XX(3)
      R2=XN**2+YN**2+ZN**2
      R=SQRT(R2)
      DO 1 I=1,7
      X(I)=XN
      Y(I)=YN
      Z(I)=ZN
      XN=XN*XX(1)
      YN=YN*XX(2)
      ZN=ZN*XX(3)
1     CONTINUE
      AA(1)=+D( 1)*Y( 1)+D( 2)*Y( 1)*Z( 1)+D( 3)*X( 1)*Y( 1)+D( 4)*X( 1)
     **Y( 1)*Z( 1)+D( 5)*Y( 1)*Z( 2)+D( 6)*Y( 3)+D( 7)*Y( 3)*Z( 1)+D( 8)
     **Y( 3)*Z( 2)+D( 9)*X( 1)*Y( 1)*Z( 2)+D(10)*X( 1)*Y( 3)+D(11)*X( 1)
     **Y( 3)*Z( 1)+D(12)*X( 2)*Y( 1)+D(13)*X( 2)*Y( 1)*Z( 1)+D(14)*X( 2)
     **Y( 1)*Z( 2)+D(15)*X( 2)*Y( 3)+D(16)*Y( 1)*Z( 3)+D(17)*X( 1)*Y( 1)
     **Z( 3)+D(18)*X( 3)*Y( 1)+D(19)*X( 3)*Y( 1)*Z( 1)+D(20)*Y( 1)*Z( 4)
```

-24-

```
*+D(21)*Y( 5)+D(22)*X( 4)*Y( 1)
 AA(1)=AA(1)+(0.0 +D(23)*Y( 1)+D(24)*Y( 1)*Z( 1)
*+D(25)*X( 1)*Y( 1)+D(26)*X( 1)*Y( 1)*Z( 1)+D(27)*Y( 1)*Z( 2)+D(28)
**Y( 3)+D(29)*Y( 3)*Z( 1)+D(30)*Y( 3)*Z( 2)+D(31)*X( 1)*Y( 1)*Z( 2)
*+D(32)*X( 1)*Y( 3)+D(33)*X( 1)*Y( 3)*Z( 1)+D(34)*X( 2)*Y( 1)+D(35)
**X( 2)*Y( 1)*Z( 1)+D(36)*X( 2)*Y( 1)*Z( 2)+D(37)*X( 2)*Y( 3)+D(38)
**Y( 1)*Z( 3)+D(39)*X( 1)*Y( 1)*Z( 3)+D(40)*X( 3)*Y( 1)+D(41)*X( 3)
**Y( 1)*Z( 1)+D(42)*Y( 1)*Z( 4)+D(43)*Y( 5)+D(44)*X( 4)*Y( 1))*EXP
*( -.06*R2)
 AA(2)=+E( 1)+E( 2)*Z( 1)+E( 3)*X( 1)+E( 4)*X( 1)*Z( 1)+E( 5)*Z( 2)
*+E( 6)*Y( 2)+E( 7)*Y( 2)*Z( 1)+E( 8)*Y( 2)*Z( 2)+E( 9)*X( 1)*Z( 2)
*+E(10)*X( 1)*Y( 2)+E(11)*X( 1)*Y( 2)*Z( 1)+E(12)*X( 1)*Y( 2)*Z( 2)
*+E(13)*X( 2)+E(14)*X( 2)*Z( 1)+E(15)*X( 2)*Z( 2)+E(16)*X( 2)*Y( 2)
*+E(17)*X( 2)*Y( 2)*Z( 1)+E(18)*Z( 3)+E(19)*Y( 2)*Z( 3)+E(20)*X( 1)
**Z( 3)+E(21)*X( 2)*Z( 3)+E(22)*X( 3)+E(23)*X( 3)*Z( 1)+E(24)*X( 3)
**Z( 2)+E(25)*Xi 3)*Y( 2)+E(26)*Z( 4)+E(27)*Y( 4)+E(28)*Y( 4)*Z( 1)
*+E(29)*X( 1)*Z( 4)+E(30)*X( 1)*Y( 4)+E(31)*X( 4)+E(32)*X( 4)*Z( 1)
 AA(2)=AA(2)
*+(0.0 +E(33)+E(34)*Z( 1)+E(35)*X( 1)+E(36)*X( 1)*Z( 1)+E(37)*Z( 2)
*+E(38)*Y( 2)+E(39)*Y( 2)*Z( 1)+E(40)*Y( 2)*Z( 2)+E(41)*X( 1)*Z( 2)
*+E(42)*X( 1)*Y( 2)+E(43)*X( 1)*Y( 2)*Z( 1)+E(44)*X( 1)*Y( 2)*Z( 2)
*+E(45)*X( 2)+E(46)*X( 2)*Z( 1)+E(47)*X( 2)*Z( 2)+E(48)*X( 2)*Y( 2)
*+E(49)*X( 2)*Y( 2)*Z( 1)+E(50)*Z( 3)+E(51)*Y( 2)*Z( 3)+E(52)*X( 1)
**Z( 3)+E(53)*X( 2)*Z( 3)+E(54)*X( 3)+E(55)*X( 3)*Z( 1)+E(56)*X( 3)
**Z( 2)+E(57)*X( 3)*Y( 2)+E(58)*Z( 4)+E(59)*Y( 4)+E(60)*Y( 4)*Z( 1)
*+E(61)*X( 1)*Z( 4)+E(62)*X( 1)*Y( 4)+E(63)*X( 4)+E(64)*X( 4)*Z( 1)
*)*EXP ( -.06*R2)
 AA(3)=+F( 1)*Y( 1)+F( 2)*Y( 1)*Z( 1)+F( 3)*X( 1)*Y( 1)+F( 4)*X( 1)
**Y( 1)*Z( 1)+F( 5)*Y( 1)*Z( 2)+F( 6)*Y( 3)+F( 7)*Y( 3)*Z( 1)+F( 8)
**Y( 3)*Z( 2)+F( 9)*X( 1)*Y( 1)*Z( 2)+F(10)*X( 1)*Y( 3)+F(11)*X( 1)
**Y( 3)*Z( 1)+F(12)*X( 2)*Y( 1)+F(13)*X( 2)*Y( 1)*Z( 1)+F(14)*X( 2)
**Y( 1)*Z( 2)+F(15)*X( 2)*Y( 3)+F(16)*Y( 1)*Z( 3)+F(17)*X( 1)*Y( 1)
**Z( 3)+F(18)*X( 3)*Y( 1)+F(19)*X( 3)*Y( 1)*Z( 1)+F(20)*Y( 1)*Z( 4)
*+F(21)*Y( 5)+F(22)*X( 4)*Y( 1)
 AA(3)=AA(3)+(0.0 +F(23)*Y( 1)+F(24)*Y( 1)*Z( 1)
*+F(25)*X( 1)*Y( 1)+F(26)*X( 1)*Y( 1)*Z( 1)+F(27)*Y( 1)*Z( 2)+F(28)
**Y( 3)+F(29)*Y( 3)*Z( 1)+F(30)*Y( 3)*Z( 2)+F(31)*X( 1)*Y( 1)*Z( 2)
*+F(32)*X( 1)*Y( 3)+F(33)*X( 1)*Y( 3)*Z( 1)+F(34)*X( 2)*Y( 1)+F(35)
**X( 2)*Y( 1)*Z( 1)+F(36)*X( 2)*Y( 1)*Z( 2)+F(37)*X( 2)*Y( 3)+F(38)
**Y( 1)*Z( 3)+F(39)*X( 1)*Y( 1)*Z( 3)+F(40)*X( 3)*Y( 1)+F(41)*X( 3)
**Y( 1)*Z( 1)+F(42)*Y( 1)*Z( 4)+F(43)*Y( 5)+F(44)*X( 4)*Y( 1))*EXP
*( -.06*R2)
 AT(1)=AA(1)
 AT(2)=AA(2)
 AT(3)=AA(3)
 RETURN
 END
```

5.2 Subroutine AXYZDN

Subroutine AXYZDN is the disturbed condition vector potential model. The routine calls subroutine SMAG which provides the correct scaling parameters for this routine. The subroutine provides the correct disturbed time vector potential at time t providing subroutine SMAG provides the correct scaling parameters. The scaling parameters that are used are STRMAG, the strength of the magnetopause currents, and SCL the size scaling parameter. These parameters are discussed in section 5.6

5.2.1 Calling Sequence

XX(3) a 3 dimension input array that specifies the position in Cartesian solar magnetic coordinates. XX(3) along the north dipole axis, XX(1) is perpendicular to XX(3) and in the plane containing XX(3) and the sun-earth line and pointing in the direction of the sun, XX(2) completes the right handed coordinate system. The distance are given in unit of Re.

AT(3) a 3 dimensioned array that returns the vector components of the disturbed condition magnetic vector potential. The units are in nanotesla-Re

T The time during the event. The time must be in units of seconds. The time, T, is passed through to SMAG, where SMAG must use it to determine the scaling parameters.

COMMON/TILTIT/TILT TILT is also an input variable. It specifies the tilt of the earth's dipole axis. Zero tilt indicates that the dipole is perpendicular to the sun-earth line. Positive tilt is when the northern dipole is tipped toward the sun. This value must be set up before a call is made to routine AXYZDN.

5.2.2 Subroutine Listing - AXYZDN

```
subroutine axyzdyn(x,a,t)
```

```fortran
C  This is the disturbed condition Vector potential.  I uses the scaling
C  algorithms developed in 1982 (JGR Aug. 82 p5943)
C  It requires that subroutine SMAG return the magnetopause current
C  and magnetopause scale size as a function of time
C  X(3) is the position in Re in solar magnetic coord
C  A(3) is the Vector potential in nanotesla-Re
C  T is the time in seconds
       REAL*8 a(3),x(3),xx(3),aa(3),STRMAG,SCL,T
       INTEGER*2 I
       call smag(strmag,scl,t)
       do 110 i=1,3
110    xx(i)=x(i)*scl
       call axyz(xx,aa)
       do 120 i=1,3
120    a(i)=aa(i)*strmag
       return
       end
```

5.3 Subroutine CURLA

This subroutine calculates the curl of the quiet time vector potential. It produces the a quiet time magnetic field model, that except for the precision in the fit and numerical derivatives will be very similar to the Olson Pfitzer 1977 tilt dependent model.

5.3.1 Calling Sequence

XX(3) a 3 dimension input array that specifies the position in Cartesian solar magnetic coordinates. XX(3) along the north dipole axis, XX(1) is perpendicular to XX(3) and in the plane containing XX(3) and the sun-earth line and pointing in the direction of the sun, XX(2) completes the right handed coordinate system. The distance are given in unit of Re.

BBB(3) a 3 dimensioned array that returns the vector components of the quiet time magnetic field. The units are in nanotesla.

COMMON/TILTIT/TILT TILT is also an input variable. it specifies the tilt of the earth's dipole axis. Zero tilt indicates that the dipole is perpendicular to the sun-earth line. Positive tilt is when the northern dipole is tipped toward the sun. This value must be set up before a call is made to routine CURLA.

5.3.2 Program Listing -- Subroutine CURLA

```
      SUBROUTINE CURLA(XX,BBB)
C  This subroutine calculates the numerical CURL of the Vector
C  potential and thus calculates the quiet time magnetic field.
C  It calls AXYZ and thus returns the value of B in nanotesla
C  XX is the Real*8 value of the position in Earth radii
C  BBB is the Real*8 value of the magnetic field in nanotesla
C  DEL is a step size parameter for the numercial CURL
      REAL*8 X(3),B(3),BB(3,3),BBB(3),xx(3)
     *,DEL
      INTEGER*2 I,J,K
      DATA DEL/0.0001/
      do 1 i=1,3
1     x(i)=xx(i)
      CALL AXYZ(X,B)
```

```
      DO 10 I=1,3
      X(I)=X(I)+DEL
      CALL AXYZ(X,BB(1,I))
10    X(I)=X(I)-DEL
      DO 20 I=1,3
      J=I+2
      J=J-(J-1)/3*3
      K=I+1
      K=K-(K-1)/3*3
20    BBB(I)=(BB(J,K)-B(J)-BB(K,J)+B(K))/DEL
      RETURN
      END
```

5.4   Subroutine DYNB

This subroutine calculates the disturbed of dynamic magnetic field values. It produces the a disturbed time magnetic field model using the curl of the vector potential.

5.4.1 Calling Sequence

XX(3) a 3 dimension input array that specifies the position in Cartesian solar magnetic coordinates. XX(3) along the north dipole axis, XX(1) is perpendicular to XX(3) and in the plane containing xx(3) and the sun-earth line and pointing in the direction of the sun, XX(2) completes the right handed coordinate system. The distance are given in unit of Re.

B(3)   a 3 dimensioned array that returns the vector components of the disturbed time magnetic field. The units are in nanotesla.

BMAG returns the magnitude of the disturbed time magnetic field in units of nanotesla

T   an input variable that gives the time during the event. This time, T, must be in units of seconds. The time, T, is passed through to SMAG, where SMAG must use the time to determine the scaling parameters.

COMMON/TILTIT/TILT TILT is also an input variable. It specifies the tilt of the earth's dipole axis. Zero tilt indicates that the dipole is perpendicular to the sun-earth line. Positive tilt is when the northern dipole is tipped toward the sun. This value must be set up before a call is made to routine ƆYNB.

5.4.2 Program Listing -- Subroutine DYNB

```
      subroutine dynb(x,b,bmag,t)
C  This is the disturbed condition magnetospheric magnetic field model
C  It determines the magnetopause magnetic field as a function of time
C  It requires that subroutine SMAG determines the magnetospheric
C  current strength and magnetospheric scaling parameter as a function
C  of time
C  X(3) is the position in Re in solar magnetic coord
```

```
C  B(3) is the mangetic field in nanotesla
C  BMAG is the mangetic field magnitude
C  T is the time in seconds
       REAL*8 x(3),xx(3),b(3),bb(3),BMAG,T,STRMAG,SCL
       INTEGER*2 I
       call smag(strmag,scl,t)
       do 210 i=1,3
210    xx(i)=x(i)*scl
       call curlA(xx,bb)
       do 220 i=1,3
220    b(i)=bb(i)*strmag
       bmag=dsqrt(b(1)**2+b(2)**2+b(3)**2)
       return
       end
```

5.5 Subroutine EFIELD

This subroutine calculates the induction electric field from the changing Chapman Ferraro currents. It produces an induction electric field as a function of time when the Chapman-Ferraro currents are changing in response to a changing solar wind pressure.

5.5.1 Calling Sequence

XX(3) a 3 dimension input array that specifies the position in Cartesian solar magnetic coordinates. XX(3) along the north dipole axis, XX(1) is perpendicular to XX(3) and in the plane containing XX(3) and the sun-earth line and pointing in the direction of the sun, XX(2) completes the right handed coordinate system. The distance are given in units of meters.

E(3) a 3 dimensioned array that returns the vector components of the disturbed time magnetic field. The units are in Volts/meter.

EMAG returns the magnitude of the disturbed time magnetic field in units of Volts/meter

T an input variable that gives the time during the event. The time must be in units of seconds. The time, T, is passed through to SMAG, where SMAG must use it to determine the scaling parameters.

COMMON/TILTIT/TILT TILT is a variable used by the vector potential program. This routine sets the value of TILT to 0. The tilt is the tilt of the earth's dipole axis. Zero tilt indicates that the dipole is perpendicular to the sun-earth line. Positive tilt is when the northern dipole is tipped toward the sun. This value must be set up before a call is made to routine EFIELD.

5.5.2 Program Listing -- Subroutine EFIELD
```
      subroutine efield(xx,E,emag,t)
C  This routine calculates the induction electric field.  It must  e used
```

```fortran
C  in MKS units.
C  XX(3) is the position is entered in meters (solar magnetic coords)
C  E(3) returns the vector induction magnetic field in Volts/meter
C     E = negative of the time derivative of the vector potential
C  Emag is the magnitude of the induction electric field.
C  T is the time in seconds.  Subroutine SMAG must be properly set up
C  to give the magnetospheric boundary parameters as a function of the
C  time in seconds
      REAL*8 X(3),XX(3),a1(3),a2(3),E(3)
      REAL*8 EMAG,T,TILT,T1,T2,DELT,CON
      INTEGER*2 I
      COMMON/TILTIT/TILT
      data con/6.371D-3/,delt/0.0001/
      do 10 i=1,3
10    x(i)=xx(i)/6.371D+6
      tilt=0
      t1=t
      t2=t1+delt
      call axyzdyn(x,a1,t1)
      call axyzdyn(x,a2,t2)
      E(1)=-(a2(1)-a1(1))/delt*con
      E(2)=-(a2(2)-a1(2))/delt*con
      E(3)=-(a2(3)-a1(3))/delt*con
      emag=dsqrt(E(1)**2+E(2)**2+E(3)**2)
      return
      END
```

5.6 Subroutine SMAG

This routine is the time dependent driver routine that must be modified by the user to give the time dependent magnetopause scaling factors. The routine must calculate the strength of the magnetopause currents, and the scale size of the magnetosphere as a function of the time, t. Time must be in units of seconds. The scale factor SCL is given by

$$SCL = 10.5/R_S$$

The magnetopause current strength factor STRMAG is given by

$$STRMAG = \left[\frac{10.5}{R_S}\right]^3$$

Where R_S is the standoff distance

5.6.1 Calling Sequence

T   is the time in units of seconds. It is passed through by the various field routines. This routine converts time to the time dependent scale factors and magnetopause current strength factor.

STRMAG returns the strength of the magnetopause current at time t

SCL   is the time dependent scale factor that scales the positions with respect to the size of the magnetopause.

5.6.2 Program listing -- Subroutine SMAG

```
      subroutine smag(strmag,scl,t)
C  This subroutine gives the standoff distance and scaling parameters
C  as a funtion of the time in seconds
      REAL*8 STRMAG,SCL,T,STDOFF
C
C  This is an example of a linear change in the standoff distance at
```

```
C     .3 Re/second
C
      goto 800
      STDOFF=10.5-.3*T
      SCL=10.5/STDOFF
      STRMAG=SCL**3
      return
C
C  This is an example of a different form for the change in magnetopause
C  configuration.  It tries to match the CRRES dB/dt observation for
C  rev 587 during the first 30 seconds of the event.
C
800   if (t.le.0)then
        strmag=1
      else
        strmag=1+9*((t/30)**1.3)
      endif
      scl=strmag**0.3333333
      stdoff=10.5/scl
      end
```

6.0 Appendix B -- Lorentz Force Integration Program

This section briefly describes a Runge Kutta trajectory integration program. It is included in this report for completeness since it was used to verify proton acceleration. It will permit any user to reproduce the values calculated in this document. The Runge-Kutta techniques used in this program are derived from a cosmic ray cut-off code that is over 20 years old. The code which was initially written to integrate the path as a function on position. The code used variable size distance steps and was written to hold the energy of a particle fixed. The code was modified to include the electric field and the distance stepping algorithm was changed to a time step code. The code has variable step size. The step size depends on the Larmor radius of the particle trajectory and the drift rate of the electric field force. The code uses MKS units throughout.

Since the program was not developed for general use, no attempt is made here to describe each of the routines in detail. The routines contain a substantial number of comment cards. This along with the overall simplicity of the code should permit most user to successfully reproduce the work in this document.

6.1   Program Listing

```
      PROGRAM TRAJCHK
C  This is a driver program that sets up a call to the trajectory program
c
      real*8 X(6),v,tilt,xmag,t
      real*4 r,xlong,th,ph,w,an1,an2,an
      integer*2 i
      common/tiltit/tilt
C  Set tilt angle to zero and request starting coords,  Enter distance in Re
c  Angle from noon is + toward +y or dusk, pitch is angle with repect to z=0
c  plane, azimuth is + toward +x
      tilt=0
```

```
      print *,'Enter R,Angle from noon,Azimuth,Pitch,W'
1005  read *,R,xlong,th,ph,W
c Tape 7 writes a file of the results, this copy is set up to inegrate
c backward in time.  To change to forward a sign must be changed in 3
c locations these are flagged by C$$$$$$$$$$$$$$$$$
      write(7,*)' Backward'
      write(7,*)r,xlong,th,ph,w
      an1=th*3.14159/180.
      an2=ph*3.14159/180
      call veloc(W,v)
      print *,w,v
      an=xlong*3.14159/180.
C Set up intial posistion X(1) thru X(3) hold particle position in meters
c X(4) thru x(6) hold particles intitial velocity in meters/second
C
      X(1)=r*6.371e+6*cos(an)
      X(2)=r*6.371E+6*sin(an)
      X(3)=0
      X(4)=cos(an1)*sin(an2)
      X(5)=sin(an1)*sin(an2)
      X(6)=cos(an2)
      xmag=dsqrt(x(4)**2+x(5)**2+x(6)**2)
      do 5 i=4,6
5     x(i)=x(i)/xmag*V
      t=30.
      CALL TRAJPRO(X,t)
      END


      SUBROUTINE VELOC(W,V)
C Determine the initial velocity of the proton given its energy in MeV
c W is the energy in MeV
c V is the velocity in meter/second
      REAL*8 V,V2C2
      V2C2=W*(W+2*931)/(W+931)**2
      V=3.0E+8*DSQRT(V2C2)
      RETURN
      END


      SUBROUTINE TRAJPRO(X,tt)
C Calculate one complete particle trajectory stating at position xx
C and time t.  XX is in meters and time is in seconds
      integer*4 n,number
      real*8 X(6),S(6),RR(6),Q(6),t,tt
      real*8 dxdt,xx,bb,bmag,e,emag,eb,RTPF,P29,OP7,DS,DT,DV,CON,
     *P5DS,P29DS,OP7DS,DIST
      integer*2 numb,i
      real*4 RRR,angle,en,xxx,xxy,xxz,xsv
      COMMON/SAD/DXDT(6),XX(6),BB(3),BMAG,E(3),EMAG,EB,t
      common/plotit/xsv(3,5000),number
      t=tt
      EB=1.
      numb=300
      number=0
      N=0
```

```
        DIST=0
        CON=.02
        DO 10 I=1,6
        XX(I)=X(I)
10      Q(I)=0
        RTPF=DSQRT(.5D0)
        P29=1.D0-RTPF
        OP7=1.D0+RTPF
        CALL EBFORCE
        EB=EMAG/BMAG
C
C  Main inegration loop  -- first set up variable step size
C  This uses Gill's method of Runge-Kutta
50      DS=CON*6.57E-8/BMAG
        DV=0.03*SQRT(XX(4)**2+XX(5)**2)
        if (eb.ne.0) then
        DT=1.05E-8/EMAG*DV
        DS=AMIN1(DS,DT)
        endif
        P5DS = .5*DS
        P29DS=P29*DS
        OP7DS=OP7*DS
C
C   GILL'S NUMERICAL INTEGRATION ROUTINE
C
        DO 60 I=1,6
        S(I) = P5DS*DXDT(I)
        RR(I)=S(I)-Q(I)
        XX(I)=XX(I)+RR(I)
60      Q(I)=Q(I)+3.*RR(I)-S(I)
        CALL EBFORCE
        DO 61 I=1,6
        S(I) = P29DS*DXDT(I)
        RR(I)=S(I)-P29*Q(I)
        XX(I)=XX(I)+RR(I)
61      Q(I)=Q(I)+3.*RR(I)-S(I)
        CALL EBFORCE
        DO 62 I=1,6
        S(I) = OP7DS*DXDT(I)
        RR(I)=S(I)-OP7*Q(I)
        XX(I)=XX(I)+RR(I)
62      Q(I)=Q(I)+3.*RR(I)-S(I)
        CALL EBFORCE
        DO 63 I=1,6
        S(I) = P5DS*DXDT(I)
        RR(I)=(S(I)-Q(I))/3.
        XX(I)=XX(I)+RR(I)
63      Q(I)=Q(I)+3.*RR(I)-S(I)
        N=N+1
        DIST = DIST + DS
C$$$$$$$$$$$ to change to forward in time change sign to  +ds
        t=t-ds
        CALL EBFORCE
        RRR=DSQRT(XX(1)**2+XX(2)**2+xx(3)**2)/6.371E+6
```

```fortran
C
C  Every so often print information on progress to the screen
       IF(N/100*100.EQ.N) then
       angle=datan2(xx(2),xx(1))*180./3.14159
       EN=(XX(4)*XX(4)+XX(5)*XX(5)+xx(6)**2)/1.912E+14
       WRITE(*,90)N,t,rrr,emag,angle,en
       endif
90     FORMAT(I7,f7.2,2f10.5,2f10.3)
C
C  Write stuff to a file every NUMB steps
       IF(N/NUMB*NUMB.EQ.N)THEN
       XXX=XX(1)/6.371E+6
       XXY=XX(2)/6.371E+6
       xxz=xx(3)/6.371e+6
       EN=(XX(4)*XX(4)+XX(5)*XX(5)+xx(6)**2)/1.912E+14
       angle=datan2(xx(2),xx(1))*180./3.14159
       WRITE (7,101) t,RRR,XXX,XXY,xxz,EN,emag,angle
       ENDIF
101    FORMAT(8f11.3)
100    FORMAT(I5,4E15.8,/,20X,3E15.8)
C  check to see if we are still in magnetosphere and that time is
C  still valid.
C  This exit condition must be changed for forward in time integration
C$$$$$$$$$$$$$$$$$$$
       IF (XXX.GT.-13.0 .and. rrr.lt.5
      *.and.t.gt.0) GOTO 50
       RETURN
       END


       SUBROUTINE EBFORCE
C  This routine calculates the Lorentz Force on a particle
C  DXDT(1),(2),(3) are the drivative of the position
C  DXDT(4),(5),(6) are the derivative of the velocity
C  all equations use MKS units
C
       REAL*8 DXDT,XX,BB,BMAG,E,EMAG,EB,t,dcon
       COMMON/SAD/DXDT(6),XX(6),BB(3),BMAG,E(3),EMAG,EB,t
C$$$$$$$$$$$  to change to forward in time make constant +
       DATA DCON/-9.5D+7/
       DXDT(1)=XX(4)
       DXDT(2)=XX(5)
       DXDT(3)=XX(6)
       CALL BFIELD(XX,BB,BMAG,t)
       call efield(xx,e,emag,t)
C$$$$$$$$$$$$$  to change to forward in time make change to +E in next 3 lines
20     DXDT(4)=DCON*(-E(1)+XX(5)*BB(3)-XX(6)*BB(2))
       DXDT(5)=DCON*(-E(2)+XX(6)*BB(1)-XX(4)*BB(3))
       DXDT(6)=DCON*(-E(3)+XX(4)*BB(2)-XX(5)*BB(1))
       RETURN
       END


       SUBROUTINE BFIELD(X,B,BMAG,t)
C  This routine combines a dipole field with a dynamic external field
C  It returns the magnetic field in MKS units (tesla)
```

```
C  XX the input position is in MKS unites (meters)
      REAL*8 X,B,BMAG,A,R,R2,t,cc,xx,btemp,bb
      integer*2 i
      DIMENSION X(1),B(1),xx(3),bb(3)
      DATA A/-8.1D+15/,cc/1.0D-9/
      do 300 i=1,3
300   xx(i)=x(i)/6.371e+6
      call dynb(xx,bb,btemp,t)
      R2=X(1)**2+X(2)**2+X(3)**2
      R=DSQRT(R2)
C  Convert external field to tesla and add dipole
      b(1)=3.d+0*x(1)*x(3)*a/(r2*r2*r)+bb(1)*cc
      b(2)=3.d+0*x(2)*x(3)*a/(r2*r2*r)+bb(2)*cc
      B(3)=(3.d+0*x(3)**2-r2)*A/(r2*R2*R)+bb(3)*cc
      BMAG=DSQRT(B(1)**2+B(2)**2+B(3)**2)
      RETURN
      END
```

6.0 Figures and Tables

Rev 587 Derivative of (B-Bmod)/Bmod   20 Second Averaging
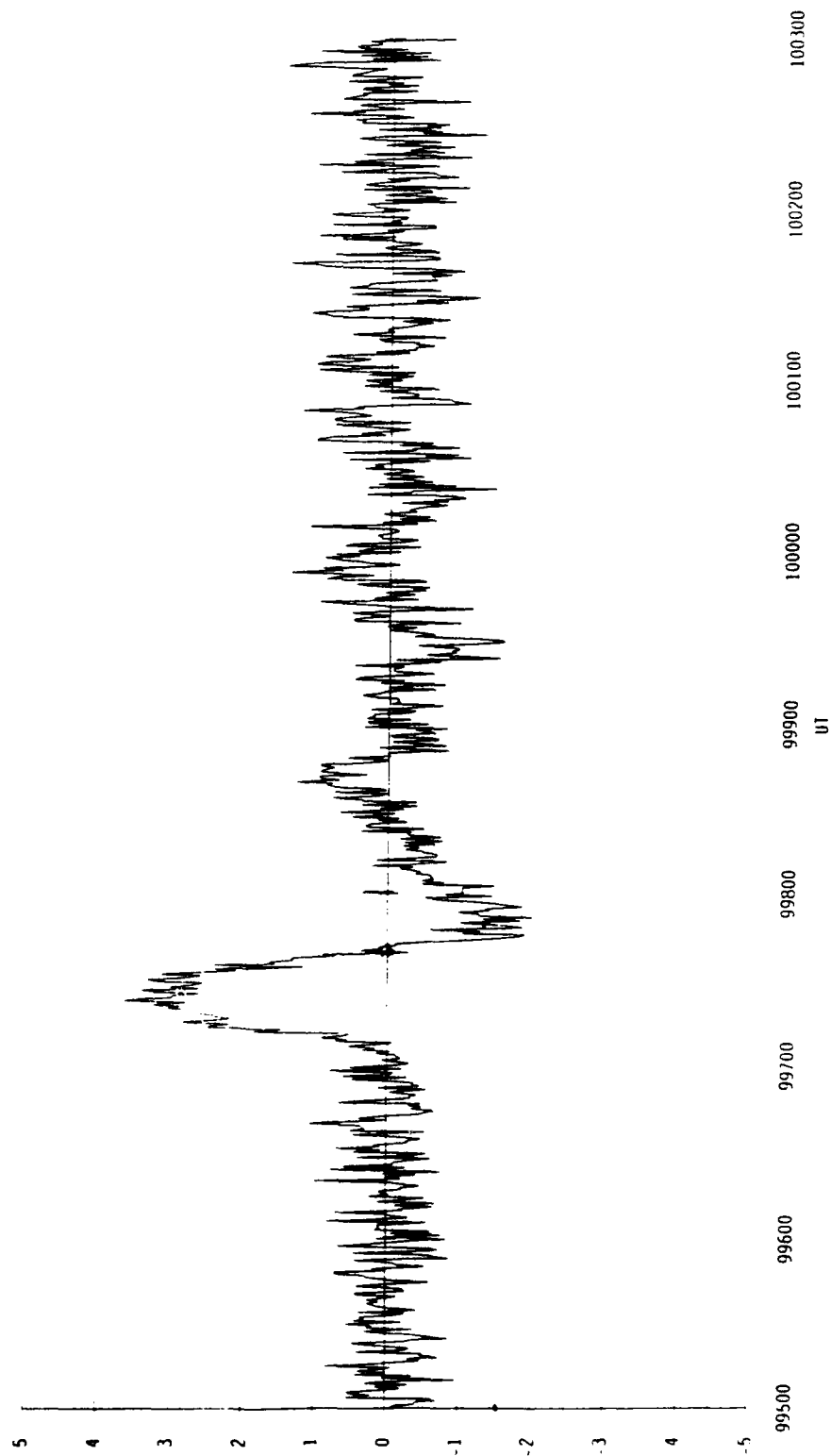
Figure 1. CRRES magnetometer data. Partial derivative with respect to time. Note: field rises rapidly with time, stays up for 30 seconds, then rate of change reverses direction but not completely.
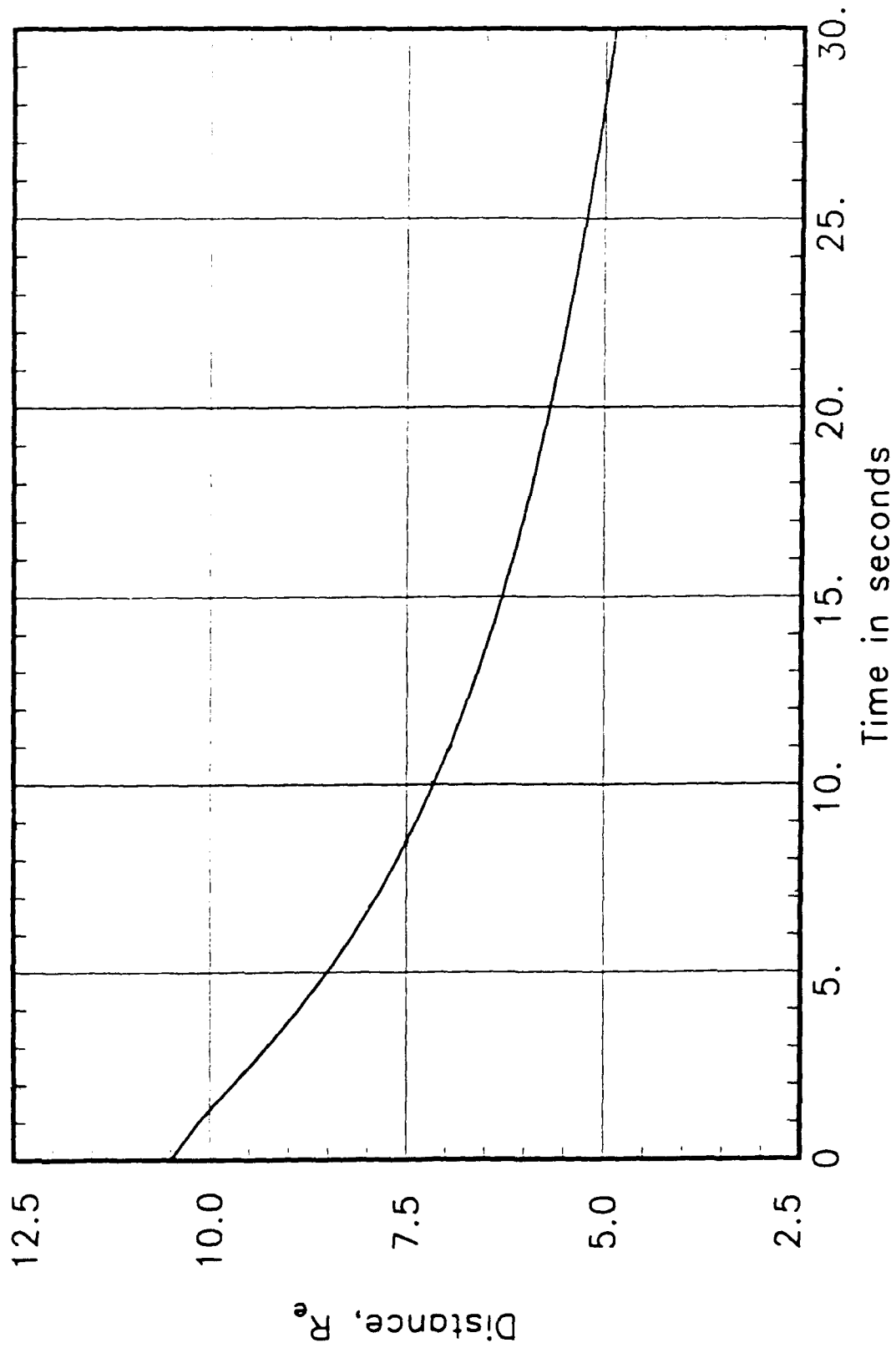
-42-

Figure 2. Standoff distance as a function of time. Rate of change of distance was adjusted to give a good fit to the rate of change of the magnetic field as observed by the CRRES magnetometer.
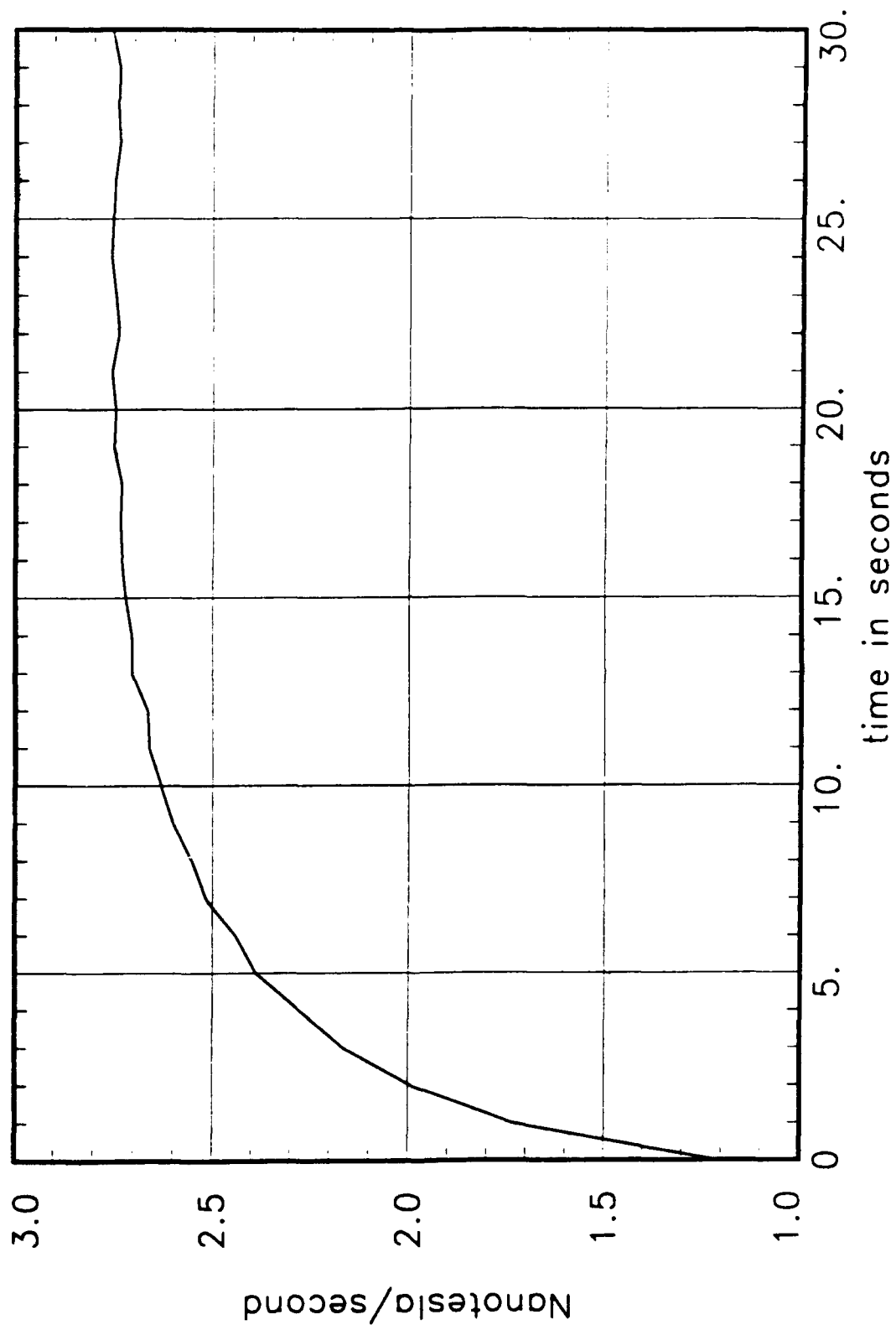
Figure 3. Time rate of change of the magnetospheric magnetic field at the location of CRRES. This field change is calculated using the standoff distance change shown in fiure 2
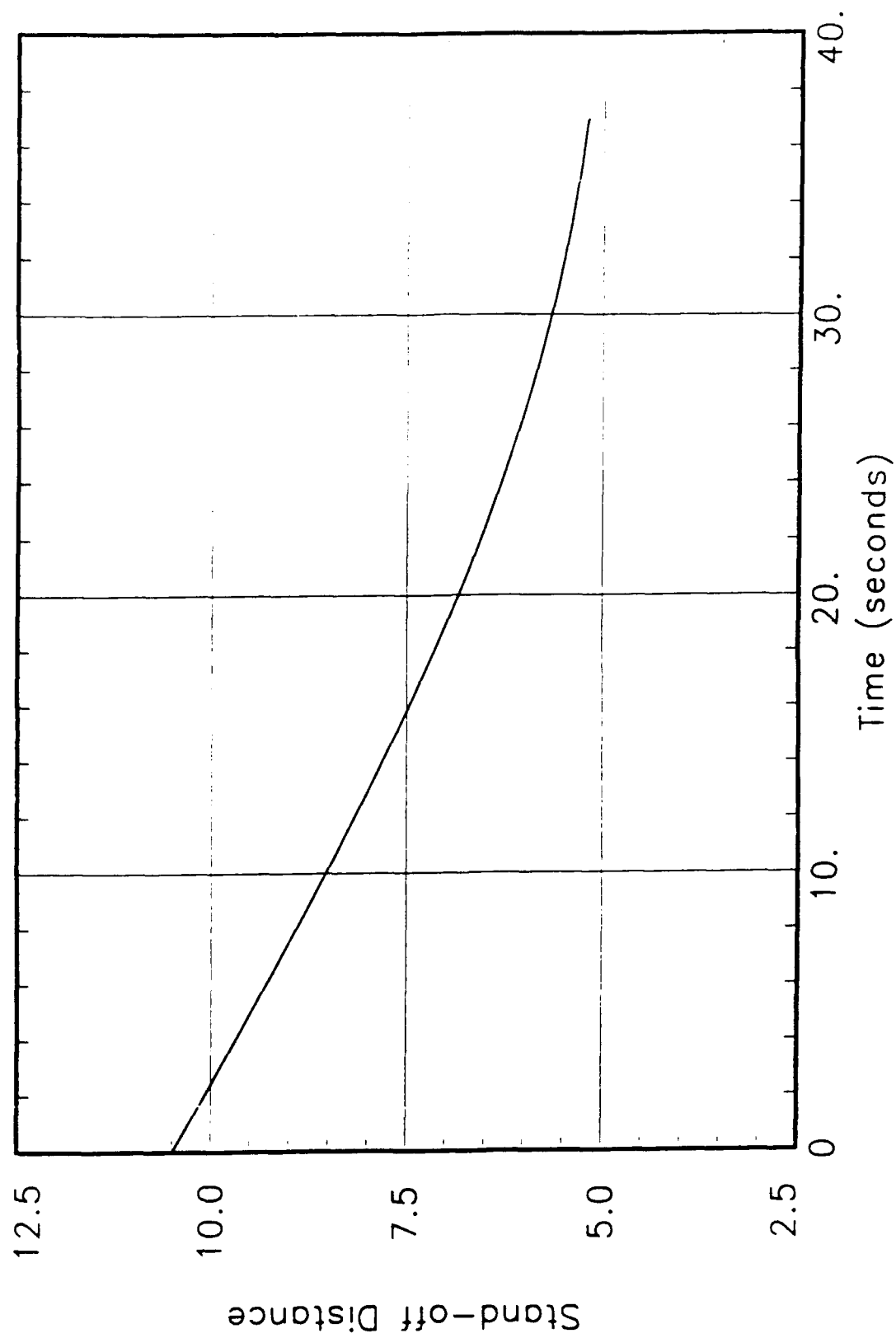
Figure 4. Time rate of change of standoff distance calculated using dynamic pressure equilibrium. Pressure balance is maintained during boundary position change
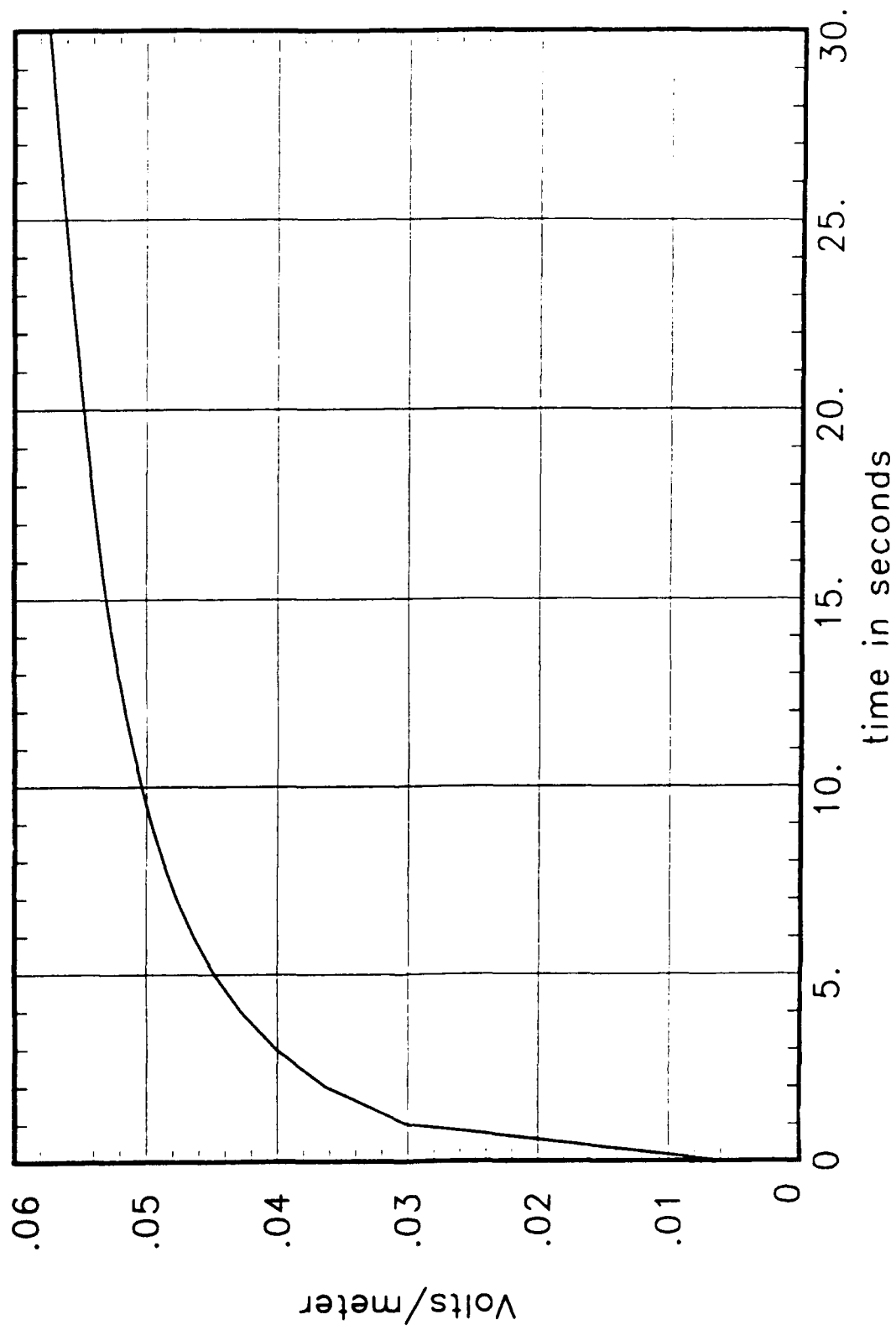
Figure 5. Induction electric field at the location of CRRES. Since CRRES is far from the boundary, the primary contribution to this change is the change in strength of the Chapman-Ferraro currents.
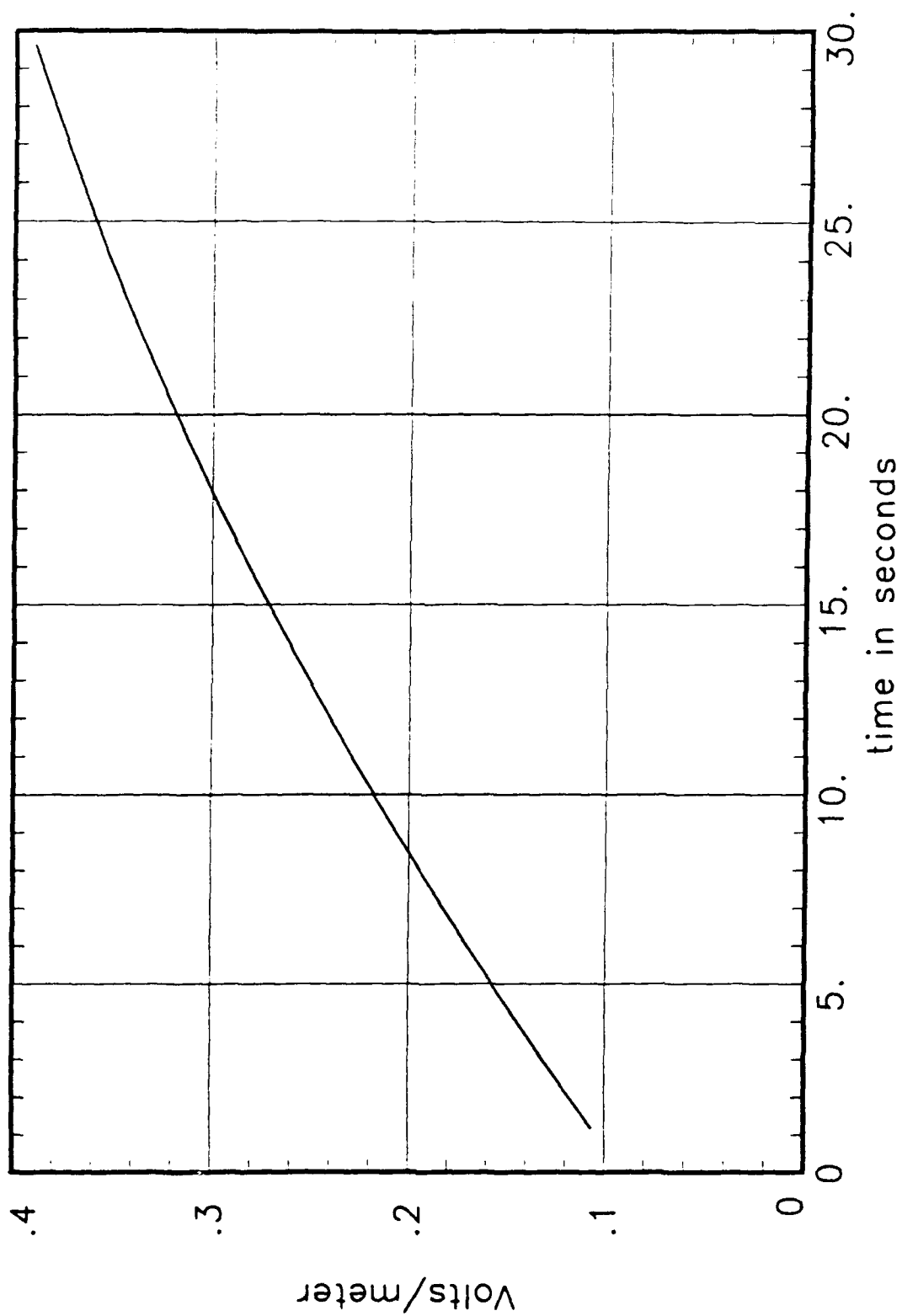
Figure 6. Induction electric field on the sun-earth line at a distance of 2.7 Re from the earth. Change is due to increase in Chapman-Ferraro currents and to the reduced distance from the observation point to the currents
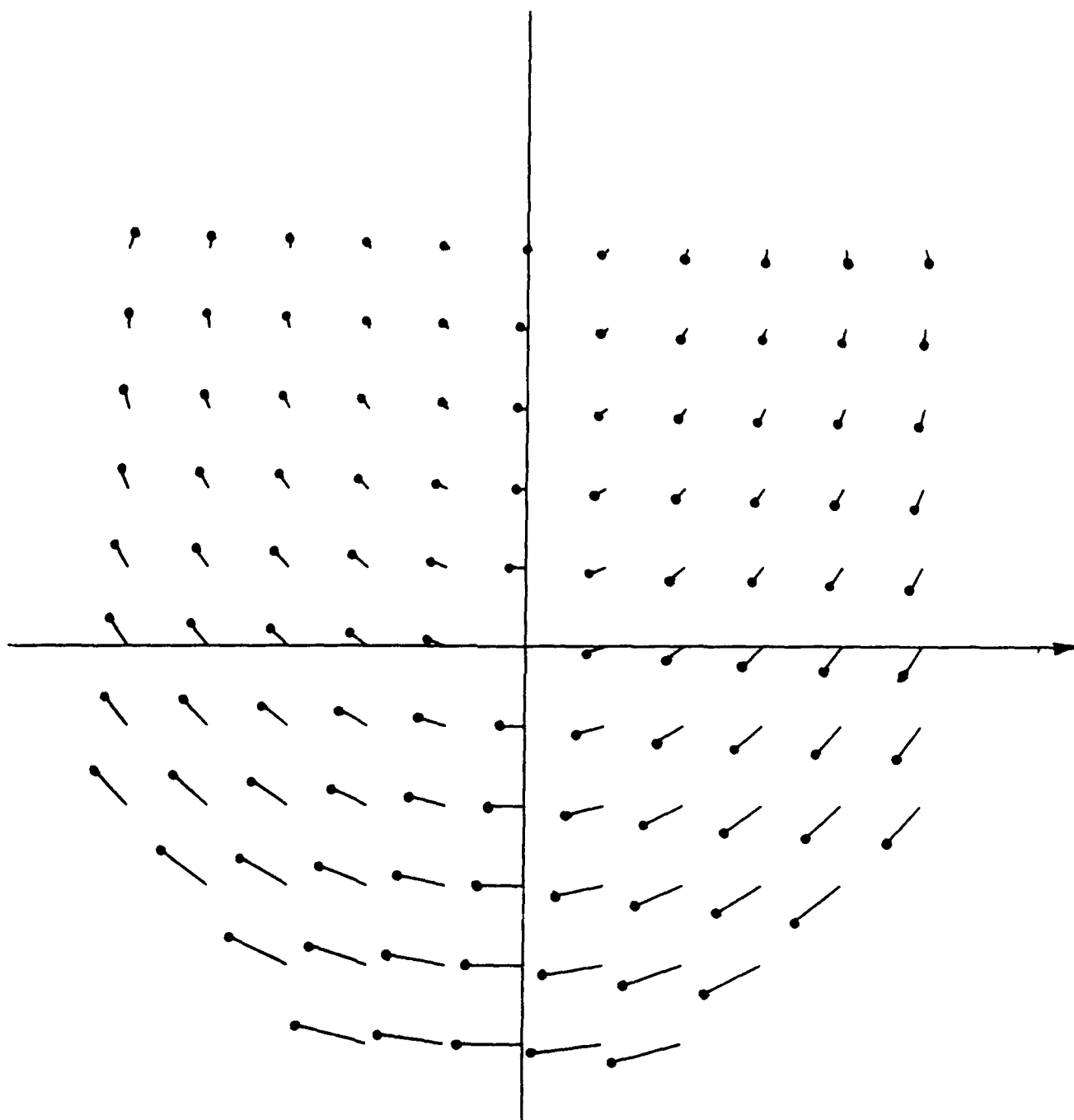
Figure 7. Electic field in the magnetic equatorial plane. Time is t = 20 seconds. Standoff distance is at 6 Re. Electric field is evaluated on a 1.0 Re grid. A vector 1.0 Re long corresponds to a field of 0.5 V/m. Dot at the head of the vector points in the direction of the field. +X is down and toward the sun.
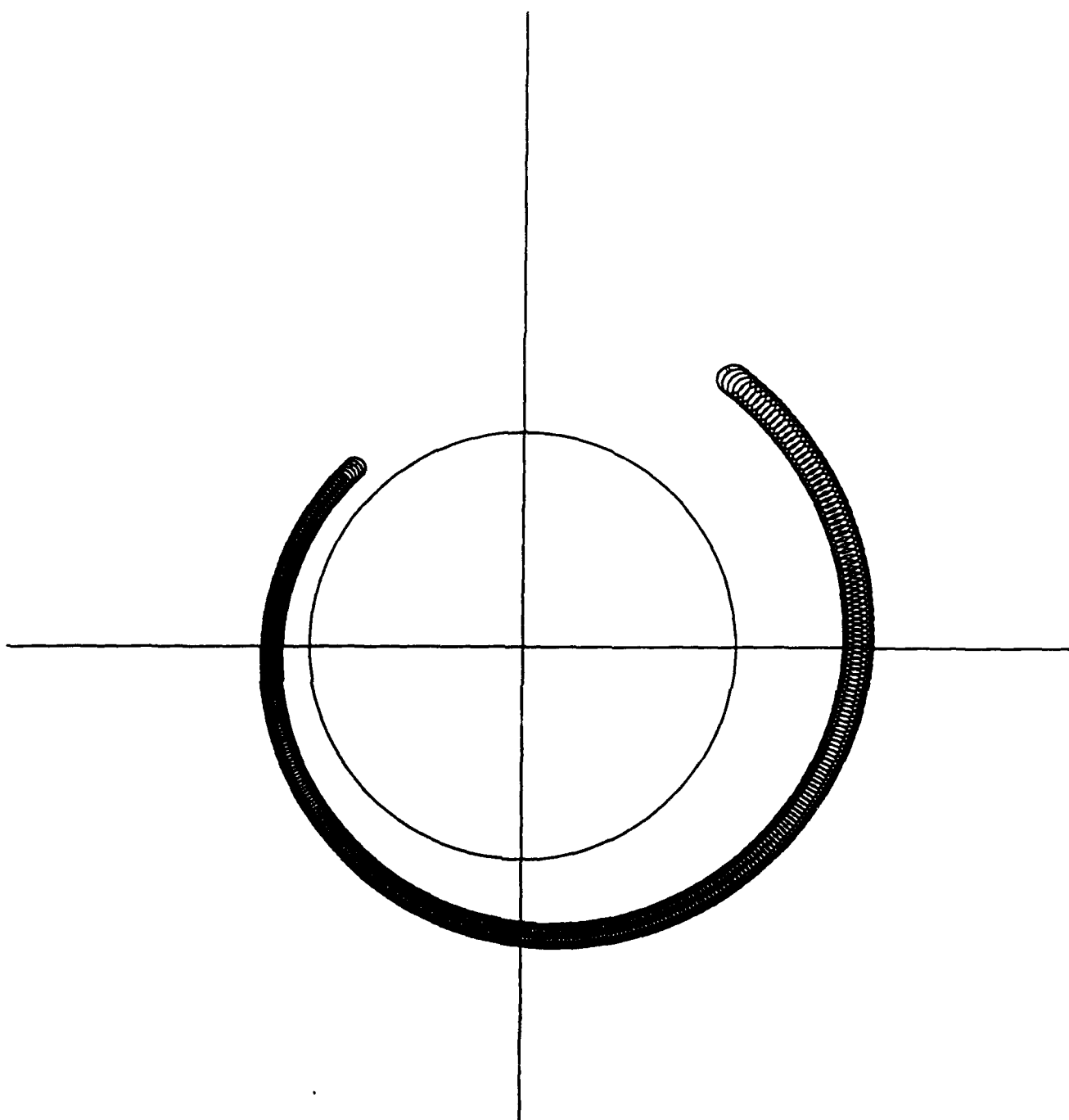
-48-

Figure 8. Sample proton trajectory. This 50 MeV proton is started at 3 hr local time at 3.0 Re. The proton trajectory is integrated backward for 30 seconds. The proton originates at a local time of about 21 hrs local time with an energy of 10 MeV. The proton gain an energy of 40 MeV. +X is down and toward the sun.

Table 1

Summary of Accelerations

Final L	Final Energy	Starting L	Starting Energy	Energy Change
2.4	50	2.9	30	20
2.4	30	2.9	15	15
2.4	10	3.0	4	6
2.7	50	3.5	20	30
2.7	30	3.7	9	21
2.7	10	3.9	2	8
3.0	50	4.5	10	40
3.0	30	4.8	6	24
3.0	10	5.0	1	9

7.0 References

McIlwain, C. E., Coordinates for Mapping the Distribution of Magnetically Trapped Particles, J. Geophys. Res., 66, 3681-3691, 1961.

Olson, W. P. and K. A. Pfitzer, Magnetospheric Magnetic Field Modeling, McDonnell Douglas Air Force Office of Scientific Research Anual Report for contract F44620-75-C-0033, January 1977,

Olson, W. P. and K. A. Pfitzer, A Dynamic Model of the Magnetospheric Magnetic and Electric Fields for July 29, 1977, J. Geophys. Res., 87, No. A8, pp. 5943-5948, August 1, 1982.

Sugiura, M., B. G. Ledley, T. L. Skillman, and J. P. Hepner, Magnetsopheric-Field Distortions Observed by OGO-3 and 5, J. Geophys. Res., 76, 7552, 1971.